

Non-dimensional analysis of cylindrical objects freely dropped into water in two dimensions (2D)

Yi Zhen^{1,2}, Xiaochuan Yu^{*3}, Haozhan Meng⁴ and Linxiong Li²

¹Natural Sciences Department, Southern University at New Orleans, New Orleans, LA, USA

²Mathematics Department, University of New Orleans, New Orleans, LA, USA

³School of Naval Architecture and Marine Engineering, University of New Orleans, New Orleans, LA, USA

⁴Department of Electrical and Computer Engineering, University of New Orleans, New Orleans, LA, USA

(Received June 11, 2020, Revised August 22, 2020, Accepted September 2, 2020)

Abstract. The dropped objects are identified as one of the top ten causes of fatalities and serious injuries in the oil and gas industry. It is of importance to understand dynamics of dropped objects under water to accurately predict the motion of dropped objects and protect the underwater structures and facilities from being damaged. In this paper, we study non-dimensionalization of two-dimensional (2D) theory for dropped cylindrical objects. Non-dimensionalization helps to reduce the number of free parameters, identify the relative size of effects of force and moments, and gain a deeper insight of the essential nature of dynamics of dropped cylindrical objects under water. The resulting simulations of dimensionless trajectory confirms that drop angle, trailing edge and drag coefficient have the significant effects on dynamics of trajectories and landing location of dropped cylindrical objects under water.

Keywords: non-dimensionalization; dropped cylindrical objects; slender body; trailing edge; offshore engineering

1. Introduction

Dropped objects are considered as one of top ten hazard accidents in the oil and gas industry and possess potential damage on offshore and onshore facilities (DORIS 2016). Dropping objects also raise the health and environmental issues in the offshore operation. ABS guidance (2017) recommends an evaluation process for the assessment of damage due to objects falling on the equipment or personnel on board. However, there is a room for the guidance to be improved by addressing the possibility of damage on structures and subsea equipment at seabed underwater caused by the dropped objects. One of the main reasons is that people are lack of knowledge of entire trajectory of dropped objects and consequently, the subsequent probability of striking additional structure and equipment and impact on other structure are not able to be estimated (ABS 2013). Therefore, it is of importance to understand the fundamental mechanism of motion of objects falling through water including prediction of their landing locations to handle the unexpected situation and reduce the harmful impact to minimum level. On this knowledge platform, one would monitor the real-time movement of dropped objects under water, predict landing location on ocean

*Corresponding author, Assistant Professor, E-mail: xyu5@uno.edu

bed and estimate the potential damage occurred. The knowledge would also benefit for proposal of guidance of offshore and onshore operation and minimize damage.

The dynamics of falling cylindrical object has been experimentally investigated. Aanesland (1987) performed two drop model tests to observe the entire trajectory from a drop at the platform deck until the object lands on the seabed. It was found that dynamics of dropped cylindrical object has similarities in maneuvering of ships (Newman 1977). Yasseri (2014) performed the experiment to investigate the landing location of fall of model-scale cylinders through water at low initial entry velocity. It was concluded that dropping cylinders have 50% of probability to fall within 10% of the water depth, 80% of probability to fall within 20%, 90% to fall within 30%, 95% to fall within 40% of water depth and 98% of probability to fall within 50% of water depth. A series of model tests have been performed by Awotahegn (2015) to study the trajectory and seabed distribution of two drill pipes with diameters 8" and 12" which fall from certain heights above the water surface. The maximum excursion points and seabed landing points have been identified and analyzed. It was found that simplified method by risk assessment of 2010 is generally conservative (DNV, 2010). The experimental trajectories of falling cylinders with various mass center, initial velocity and drop angle have been reported (Kim *et al.* 2002).

The costs of experimental studies lead the research to focus on development of numerical simulations of hydrodynamic analyses of motion of slender body under water (Bergmann and Iollo 2011). Two-dimensional motion of falling objects is simulated by solving the differential equations of motion (Luo and Davis 1992). A computer program called DELTA is used to study the effects of several parameters. It was found that the drop angle has significant effect on horizontal excursion at the seabed level. Moreover, both drop height and angle affect the horizontal velocity of the object. In addition, the tangential drag coefficient seemed to have little impact on the trajectory. Using the same computer program, DELTA, multiple numerical studies on trajectories of two dropped drill casings have been carried out (Colwill and Ahilan 1992). These studies confirmed that drop height above waterline and initial dropped angle were critical parameters affecting the horizontal velocity. It is successfully established the relation between impact velocity and probability of its exceedance based on the findings of reliability-based impact analysis. Characteristic motions of freely falling body through water has been studied (Chu *et al.* 2005). The time-dependent six degrees of freedom motions of dropping object in water has been obtained by numerical solution scheme. The viscous effect has been considered on trajectory of cylindrical body by estimating the drag coefficients of the bodies for various body aspect ratios, end shapes, and orientations to incoming flow. Comparison between numerical results and experimental tests indicate that simulated dynamic pattern is affected significantly by initial drop angle, body aspect ratio, and mass center. Simulation program IMPACT 35 has been developed to simulate falling objects' movement through a single fluid such as air, water or sediment and motion through the interface of different fluids. In rotational coordinate system, equations of motion are formed by linearization of drag, lift force, and moments with temporally varying coefficients in time domain (Chu *et al.* 2005, Chu *et al.* 2006). IMPACT35 has been validated by comparison between its results and experimental data. Nonlinear dynamic simulation of dropped objects has been presented and a detailed accurate assessment of dropped object trajectories has been obtained by incorporating detailed hydrodynamic models of complex geometries. Moreover, the entire impact zone is determined by Monte-Carlo simulations that consider the objects' initial drop angle as random variables (Majed and Cooper 2013, Xiang *et al.* 2016). A different model of falling cylindrical object has been proposed by considering the effect of axial rotation, and simulated trajectory has been obtained by modified maneuvering equations for a slender rigid body (Xiang *et al.* 2016, Xiang *et al.* 2017a, Xiang *et al.* 2017b), and a numerical tool

called Dropped Objects Simulator (DROBS) has been successfully developed. It should be addressed that the numerical results from DROBS have been validated by at least two experimental tests, implemented by Aanesland (1987) and Chu *et al.* (2005), respectively. DROBS was successfully applied to investigate the random distribution of a dropped model rocket freely falling into the UNO's towing tank (Yu *et al.* 2020b). It was used to study the hit probability of dropped cylindrical objects hit probability on pipelines at seabed in offshore operations (Yu *et al.* 2020a), and the results from DROBS were compared with those based on simplified method (DNV 2010). It was found that such a simplified method may introduce larger errors to the calculation of hit probability and mean radii.

In this paper, the trajectories of small-scaled hollow drill pipes are calculated by DROBS. The differential equations of motion in this paper are solved by ODE45 solver of Matlab, which represents a fourth-order Runge-Kutta scheme. Firstly, the non-dimensionalization is carried out for the equations of motion of surge-heave-pitch motion of dropped cylindrical objects. The simulated results agree well with dimensionless data from model tests (Aanesland 1987). Then, the dimensionless dynamic equations are used to re-investigate various factors that may affect the trajectories such as trailing edge, drag coefficient and drop angle. Finally, simulated trajectories in X-Z plane are obtained at a 0.8 dimensionless water depth by varying the drop angle.

2. Non-dimensionalization of equations of motion in two dimensions (2D) for dropped cylindrical objects

2.1 Equations of motion in 2D and hydrodynamic force components

Aanesland (1987) proposed the two-dimensional equations to numerically describe the motions of falling drilling pipes by modifying maneuvering equation of ships. Based on the observation of his model tests of dropping pipe through water, it was found that there was similarity between the motion of dropping pipe and maneuvering of slender ships (Newman 1997). The slenderness means the length of objects exceed its diameter by an several order of magnitude. For dropped pipe, the length of pipe is far greater than its diameter. Thus, the dropped pipe was theoretically treated as a slender body. During the large part of motion under water, the longitudinal velocity dominated the lateral velocity and the coupled surge-heave-pitch motion of the dropped pipe corresponded to the coupled surge-sway-yaw motion of the ship.

As shown in Figure, the upper-case letters X and Z denote a global coordinate system. X-axis represents the coordinate of the still-water surface. The Z-axis represents the coordinate along the vertical direction and upward is defined as positive direction. The local coordinate system denoted by lower case letters x and z is fixed on the dropped cylindrical object. The x-axis describes the cylinder axis and origin is defined at the center of gravity. The local coordinate coincides with global coordinate system where the cylinder positions horizontally on the water surface. The β denotes the instantaneous angle between the x-axis of the local coordinate system and the X-axis of the global coordinate system.

The parameters included in the dynamic equations are referred to the local coordinate system (x, z) and the cylinder is assumed moving as a rigid body. In addition, the shape of cylinder is assumed symmetric about the center of gravity in present study ($x=z=0$).

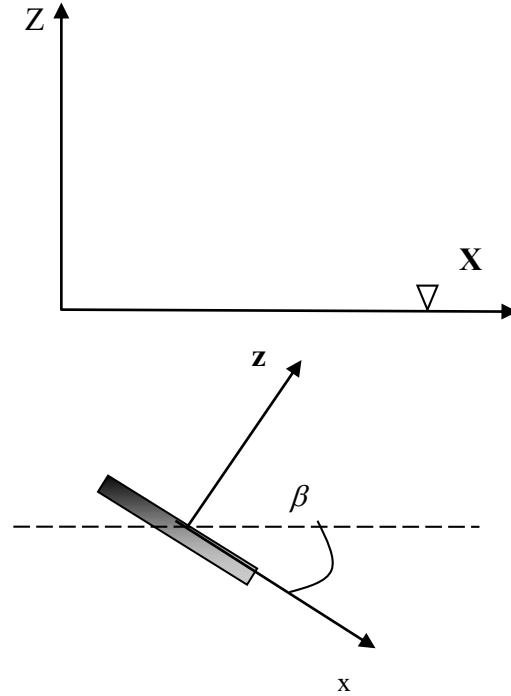


Fig. 1 The local and global coordinate systems for dropped cylindrical object

Suppose the velocity of surge is U_1 , velocity of heave motion U_3 and pitch motion Ω_2 , then the equations of motion are given in

$$(m - \rho \nabla) g \sin(\beta) + F_{dx} = m \dot{U}_1 \quad (1)$$

$$-(m - \rho \nabla) g \cos(\beta) + F_{dz} = [U_1 m_t U_3 - U_1 (x_t m_t) \Omega_2 + m_{33} \dot{U}_3] + m(\dot{U}_3 - U_1 \Omega_2) \quad (2)$$

$$M_{dy} = [-U_1 (m_{33} + x_t m_t) U_3 + U_1 x_t^2 m_t \Omega_2 + m_{55} \dot{\Omega}_2] + M_{55} \dot{\Omega}_2 \quad (3)$$

where the parameters are defined as follows:

β : the instantaneous rotational angle between x-axis and X-axis

m : the mass of cylinder

D: diameter of the cylinder

ν : kinematic viscosity of water

L: length of the cylinder

g : gravitational acceleration

ρ : the density of water

∇ : the volume of the cylinder

M_{55} : moment of inertia in pitch direction

m_{55} : added mass for pitch motion from strip theory

m_{33} : added mass for heave motion from strip theory

m_t : 2D added mass coefficient for heave direction at the trailing edge

x_t : longitudinal position of effective trailing edge

C_{dx} : drag coefficient in x-direction

C_{dz} : drag coefficient in z-direction

The viscous forces F_{dx} , F_{dz} and the moment M_{dy} are evaluated with

$$F_{dx} = 0.664\pi U_1 \sqrt{|U_1|} \sqrt{\nu \rho^2 L} + \frac{1}{8} \rho \pi C_{dx} D^2 U_1 |U_1| \quad (4)$$

$$F_{dz} = \frac{1}{2} \int_{-0.5L}^{0.5L} \rho C_{dz} D U_z(x) |U_z(x)| dx \quad (5)$$

$$M_{dy} = -0.5 \int_{-0.5L}^{0.5L} \rho C_{dz} D x U_z(x) |U_z(x)| dx \quad (6)$$

In Eq. (1), no added mass is considered in surge motion because the added mass of a slender body in the longitudinal direction is negligible compared with the body mass (Newman 1977). Eq. (4) represents the drag forces along x-direction and it includes two types of drag. The first term is friction drag which can be obtained from boundary layer theory for laminar flow (Schlichting 1979). The second term is form drag (Hoerner 1958). Eq. (5) is drag force along z-direction in local coordinate system. Eq. (6) denotes the torque about y-axis (Gudmestad and Moe 1996). U_z is the local relative velocity in z-axis direction between cylinder and water. It may be approximated by $-(U_3 - \Omega_2 x)$, $-0.5L < x < 0.5L$.

After solving for U_1 , U_3 and Ω_2 in the local coordinate system at each time step, the motions in the local coordinate system are transformed into the motions in the global coordinate system by using the relationship

$$\begin{bmatrix} \dot{X} \\ \dot{Y} \end{bmatrix} = \begin{bmatrix} U_1 & U_3 \end{bmatrix} \begin{bmatrix} \cos(\beta) & -\sin(\beta) \\ \sin(\beta) & \cos(\beta) \end{bmatrix} \quad (7)$$

The instantaneous angle β is solved by $\dot{\beta} = \Omega_2$.

2.2 Non-dimensionalization of equations of motion

To obtain the units of measurement of the velocity U and time T , the governing equation of surge motion Eq. (1) is used. By introducing the dimensionless velocity U' and dimensionless time t' ,

the velocity of surge motion U_1 and time t can be expressed as

$$U_1 = U U_1'$$

$$t = T t'$$

where U_1' and t' are the dimensionless surge velocity and dimensionless time, respectively. Plugging the expressions above into equation of surge motion Eq. (1), we have

$$(m - \rho \nabla) g \sin(\beta) - 0.664 \pi \sqrt{v \rho^2 L} U_1' \sqrt{|U_1'|} U^{3/2} - 0.125 \rho \pi C_{dx} D^2 U_1' |U_1'| U^2 = m \dot{U}_1' \frac{U}{T} \quad (8)$$

Dividing by $m \frac{U}{T}$ on both sides of Eq. (8), we have

$$\dot{U}_1' = \frac{m - \rho \nabla}{m} g \sin(\beta) \frac{T}{U} - 0.664 \pi \sqrt{v \rho^2 L} U_1' \sqrt{|U_1'|} U^{3/2} \frac{T}{mU}$$

$$- 0.125 \rho \pi C_{dx} D^2 U_1' |U_1'| U^2 \frac{T}{mU}$$

Choosing

$$0.125 \rho \pi D^2 U^2 \frac{T}{mU} = 1 \quad \text{and} \quad g \frac{T}{U} = 1$$

Thus, the unit of measurement of velocity and time in trajectory of dropped cylindrical object are obtained as

$$U = \sqrt{\frac{8mg}{\rho \pi D^2}},$$

and

$$T = \sqrt{\frac{8m}{\rho g \pi D^2}} \quad (9)$$

Using unit of measurement of velocity and time U and T in Eq. (9), the dynamic equations of surge, heave and pitch motions in the two-dimensional theory for dropped cylindrical objects can be non-dimensionalized to Eqs.(10)-(12), respectively. From the dimensionless equations, the parameters in the mathematical models are reduced comparing with Eqs. (1)-(3). In surge motion, the parameters are reduced from nine to three. The parameters have been reduced from ten to five in heave motion. Non-dimensionalization reduce parameter in pitch motion from eight to three.

For surge motion

$$\dot{U}_1' = A_1 \sin(\beta) - B_1 U_1' \sqrt{|U_1'|} - C_1 U_1' |U_1'| \quad (10)$$

where U'_1 is dimensionless velocity of surge motion and A_1 , B_1 , and C_1 dimensionless coefficients which are

$$A_1 = \frac{m - \rho \nabla}{m},$$

$$B_1 = 0.664 \pi \sqrt{\nu \rho^2 L} U_1^{1/2} \frac{T}{m},$$

and $C_1 = C_{dx}$

For heave motion

$$\dot{U}'_3 = -A_2 \cos(\beta) + B_2 U_3'^2 + C_2 \Omega_2'^2 + D_2 U_1' U_3' + E_2 U_1' \Omega_2' \quad (11)$$

where U'_3 and Ω'_2 are dimensionless velocity of heave motion and dimensionless angular velocity about y-axis and A_2 , B_2 , C_2 , D_2 and E_2 are dimensionless coefficients which are defined as below

$$A_2 = \frac{m - \rho \nabla}{m_{33} + m},$$

$$B_2 = 0.5 \rho C_{dz} DLUT / (m_{33} + m),$$

$$C_2 = 0.5 \rho C_{dz} DL^3 / UT / (m_{33} + m),$$

$$D_2 = m_t UT / (m_{33} + m),$$

$$E_2 = (x_t m_t + m) / (m_{33} + m)$$

For pitch motion

$$\dot{\Omega}'_2 = A_3 U_1' \Omega_2' + B_3 U_1' U_3' + C_3 U_1' \Omega_2' \quad (12)$$

where U'_1 , U'_3 , and Ω'_2 are dimensionless velocity of surge motion, heave motion and dimensionless angular velocity about y-axis, respectively. The dimensionless coefficients A_3 , B_3 , and C_3 are

$$A_3 = 0.5 \rho C_{dz} DL^3 UT / (m_{55} + M_{55})$$

$$B_3 = (m_{33} + x_t m_t) (UT)^2 / (m_{55} + M_{55}),$$

and $C_3 = -x_i^2 m_i UT / (m_{55} + M_{55})$.

The unit of measurement of length scale L can be obtained by unit of measurement of velocity and time

$$L = UT = \sqrt{\frac{8mg}{\rho\pi D^2}} \sqrt{\frac{8m}{\rho g \pi D^2}} = \frac{8m}{\rho\pi D^2} \quad (13)$$

The length L is the distance covered in the time interval of T at the velocity U. It will be used to estimate the order of magnitude of the distance at which oscillating motion of dropped cylindrical object terminates.

3. Case study

3.1 Effects of hydrodynamic force and moments on motions

Using the proposed units of measurement of velocity and time in the Eq. (9), the two-dimensional dynamics can be written in dimensionless forms of Eqs. (10)-(12). For surge motion, dimensionless friction drag and dimensionless form drag are plotted in Figs. 2 at initial dropping angles of 30°. From the figures, the magnitudes of friction drag are greater than those of form drag. The friction drag seems dominant. Furthermore, Figs. 2-4 show that friction drag and form drag are oscillating force, and their magnitude decreases in time frame. For heave motion, dimensionless viscous force F_{dz} and dimensionless hydrodynamic force induced by the effective trailing edge $F_7 = D_2 U_1' U_3' + E_2 U_1' \Omega_2'$ are plotted in Figs. 3 and 4. It can be seen that viscous force and trailing edge force are in opposite direction. When the initial dropping angle increases, the magnitudes increase. However, their magnitudes are roughly same. Furthermore, figures show that friction drag and form drag are oscillating force and their magnitude decreases in time frame. For pitch motion, dimensionless moment induced by viscous force and hydrodynamic force induced by the effective trailing edge are considered. Magnitude of moments induced by viscous force and hydrodynamic force are in the same level. When the initial dropping angle increases, the initial magnitudes of moments increase. However, their magnitudes decay faster with increasing in dropping angle. Furthermore, Fig. 2 shows that friction drag and form drag are oscillating, and their magnitude decreases in time frame. Comparing effect of force and moment, moment is dominating in motion of dropped cylindrical object.

For scaled model (1:20.32), specifications are: length=0.45 meters, density=0.548 kg/m³, mass=0.247 kg, diameter of cross-sectional area=0.01 meters, and The density of water =1025 kg/m³. The units of measurement of velocity and time can be obtained through Eq. (9) as velocity U=7.83 m/s and time T=0.78s. Based on proposed units of velocity and time, the dimensionless coefficients in equations of surge, heave, and pitch motions can be evaluated and are shown in Tables 1-3. From the Table 1, it can be seen that the effect of friction drag which is obtained from boundary layer theory for laminar flow is dominant in the surge motion. Table 2 shows that drag force described by Morison equation is the most important for heave motion. Table 3 indicates that the most contributions to moments for pitch motion come from torques caused by drag force described by Morison equation and hydrodynamic force.

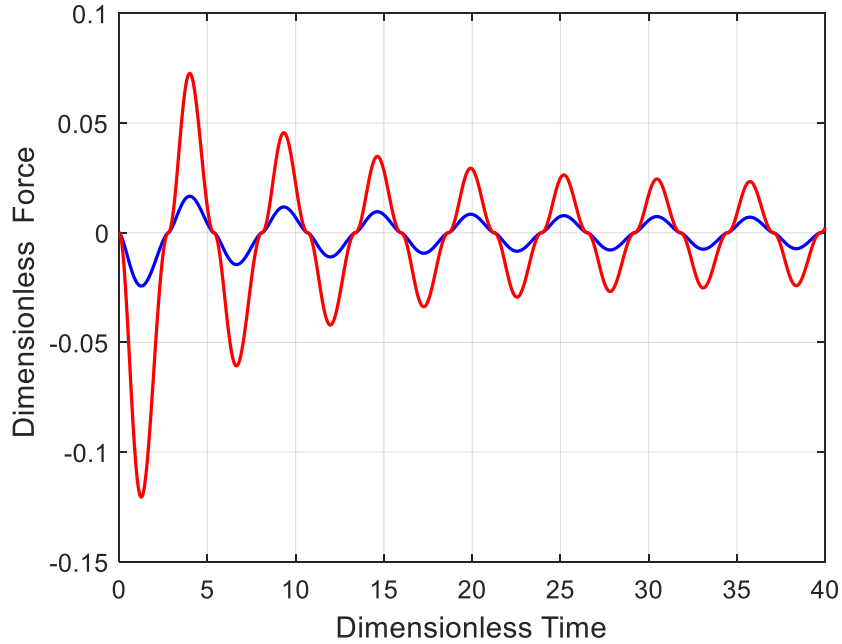


Fig. 2 Dimensionless friction drag (red line) and form drag (blue line) at drop angle 30°

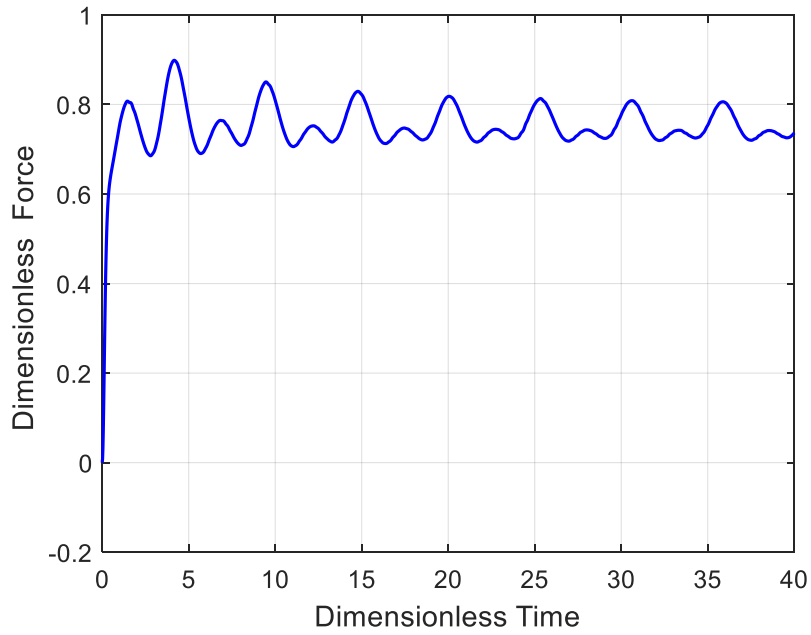


Fig. 3 Dimensionless force F_{dz} described by Morison's equation at drop angle 30°

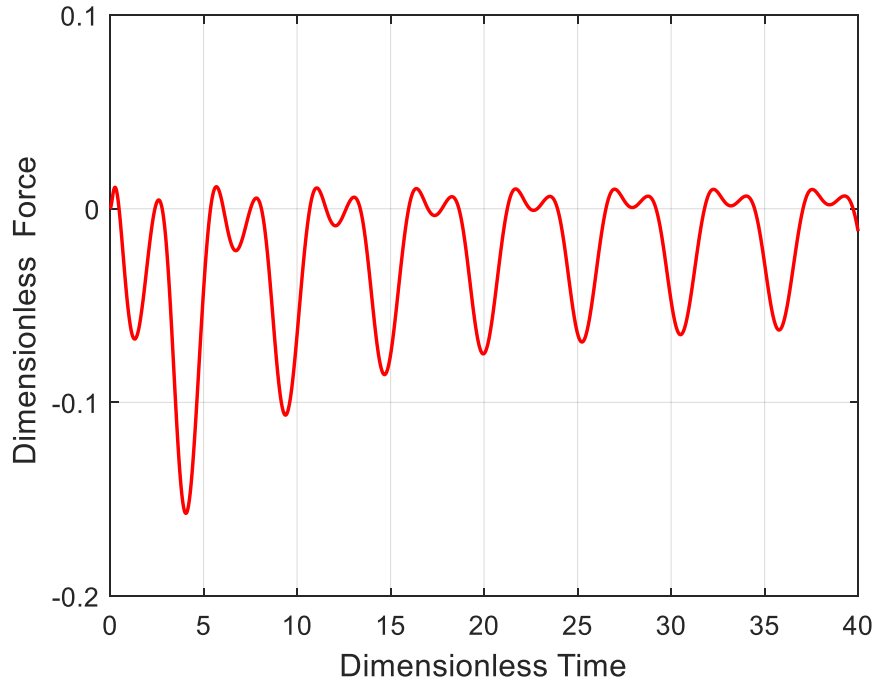


Fig. 4 Dimensionless force F_T induced by trailing edge at drop angle 30°

Table 1 The values of dimensionless coefficients for surge motion

Dynamic component	Dimensionless coefficients	Value
Hydrostatic force	A_1	0.85
Friction drag	B_1	12.71
Form drag	C_1	1.1-1.3

Table 2 The values of dimensionless coefficients for heave motion

Dynamic component	Dimensionless coefficients	Value
Hydrostatic force	A_2	0.74
Drag force	B_2	49.81
Drag force	C_2	0.27
Hydrodynamic force	D_2	0.001
Hydrodynamic force	E_2	0.87

Table 3 The values of dimensionless coefficients for pitch motion

Dynamic component	Dimensionless coefficients	Value
Drag moment	A_3	597.96
Hydrodynamic moment	B_3	283.11
Hydrodynamic moment	C_3	0.001

3.2 Simulated trajectories vs. experimental envelop

Using non-dimensional governing equations of surge, heave and pitch motions, dimensionless simulations have been performed through the use of the trailing edge values of $Xt=0.0, 0.3, 0.4$ and 0.5 . Trailing edge is rear edge of the cylinder and of prime importance in dynamics of cylinder because the position of trailing edge directly affects force and moment in heave and pitch motions, respectively. Resulting non-dimensional trajectories are shown in Figs. 5-7 for the initial orientation angles of $\theta_0=30^\circ, \theta_0=45^\circ$, and $\theta_0=60^\circ$, respectively. For both initial angles of $\theta_0=30^\circ$ and $\theta_0=45^\circ$, the simulated dimensionless trajectories at the trailing edge positions $Xt=0.3$ and $Xt=0.4$ are more in line with the experimental results. Dimensionless trajectories with $Xt=0.5$ overshoot the right-hand side boundary of the observed experimental range. All trajectories show a similar pattern. The effect of the trailing edge decreases at a larger initial orientation angle θ_0 . Fig. 5 shows the simulated dimensionless trajectories for $\theta_0=30^\circ$. The simulated dimensionless trajectory for $Xt=0.4$ seems to agree well with of dimensionless experimental values. From Fig. 5 to Fig. 7, it can be seen that when initial orientation angles increase from 30° to 60° , simulated dimensionless landing points seem to shift to farther landing location along horizontal direction. Landing positions of the dropped cylindrical at large initial dropping angles seem to separate farther apart compared with those at lower angles. The dimensionless simulations show that the trailing edge position Xt has a significant effect on the simulated dimensionless trajectory which can lead to differences between experimental and numerical trajectories shown in Figs. 5-7. The trailing edge position Xt has an appropriate range which depends on the magnitude of initial drop angle.

Figs. 8-10 show the resulting non-dimensional trajectories for different z directional drag coefficients, $C_{dz}=1.0, 1.1, 1.2$ and 1.3 , respectively. Fig. 8 shows that simulated dimensionless trajectory overshoot at right boundary of experimental envelop for all values of C_{dz} at drop angle of 30° . From Fig. 9, It can be seen that dimensionless trajectories for $C_{dz}=1.0$ and 1.1 are in line with experimental envelop when the drop angle is increased to 45° . When the drop angle is increased to 60° , the dimensionless trajectories for $C_{dz}=1.2$ and 1.3 seem to fall into the range of experimental dimensionless trajectory as shown in Fig. 10. Overall, it can be seen that for each drop angle, the dropped object demonstrated similar simulated dimensionless trajectories compared with simulation with physical units. It shows that trajectory under the larger drag coefficient C_{dz} seems to cause farther landing point in positive x -direction. The possible reason is that larger C_{dz} arises larger resistance force which slows down the falling motion and allows the dropped cylindrical object to travel further in X -direction.

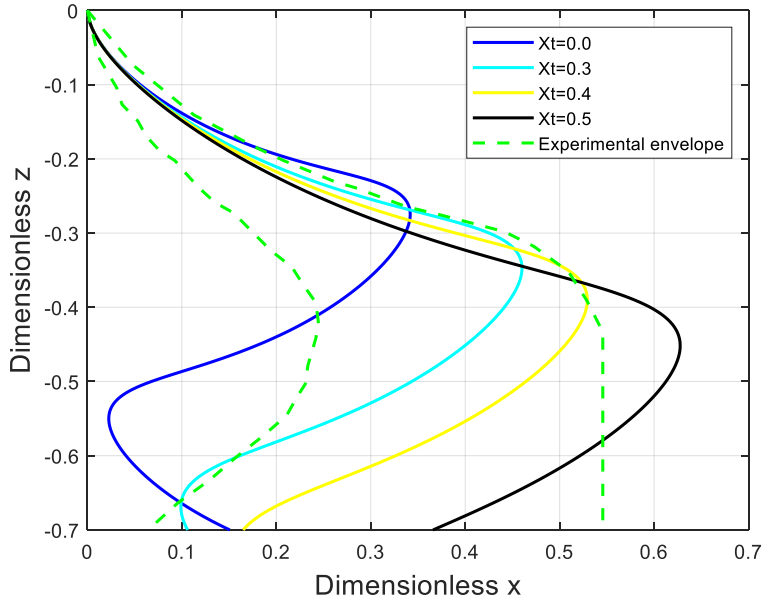


Fig. 5 Simulated dimensionless trajectories at drop angle 30° with different trailing edge coefficient

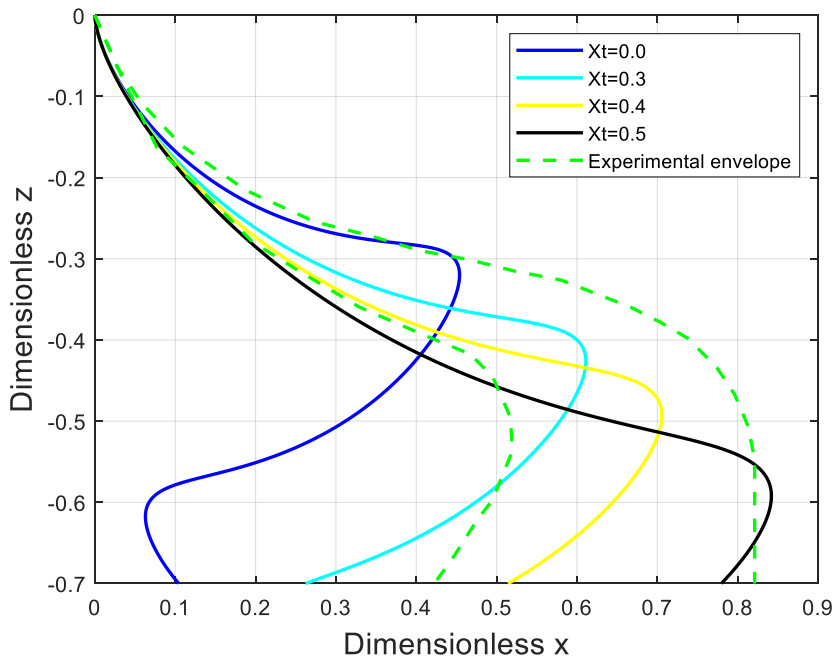


Fig. 6 Simulated dimensionless trajectories at drop angle 45° with different trailing edge coefficient

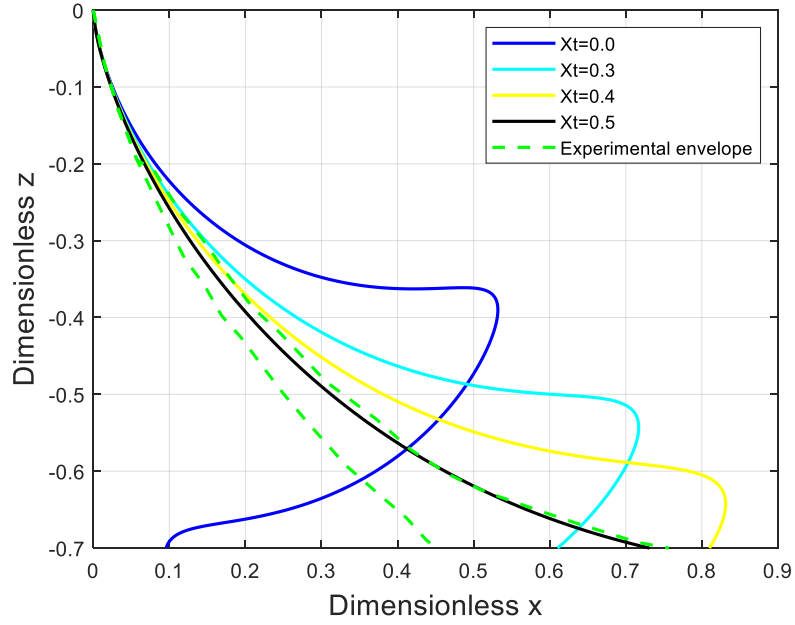


Fig. 7 Simulated dimensionless trajectories at drop angle 60° with different trailing edge coefficient

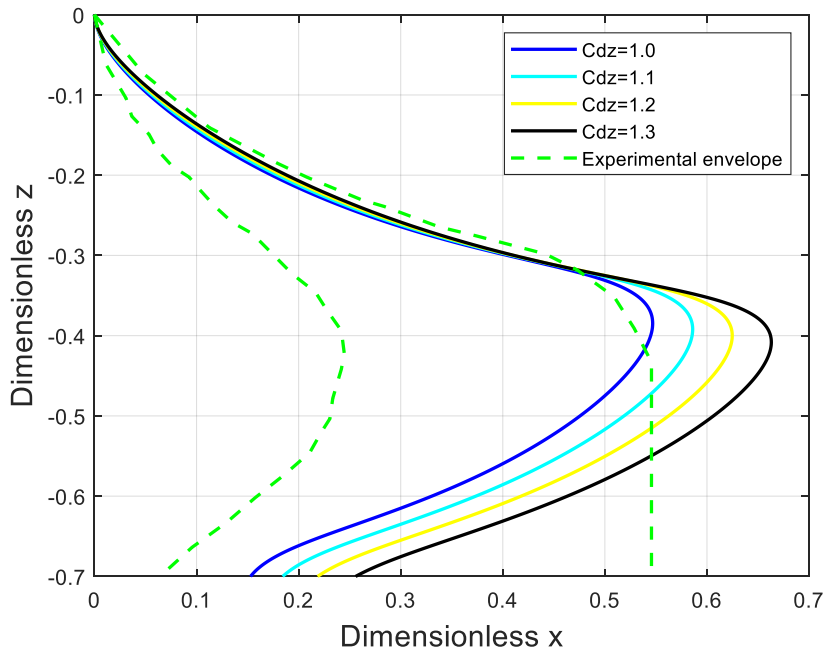


Fig. 8 Simulated dimensionless x - z plane trajectories with different C_{dz} at drop angle 30°

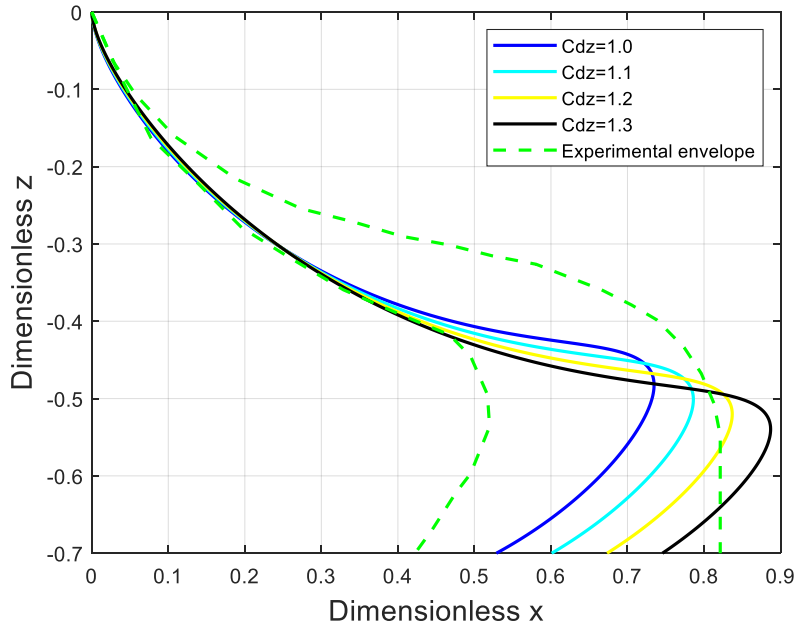


Fig. 9 Simulated dimensionless x-z plane trajectories with different C_{dz} at drop angle 45°

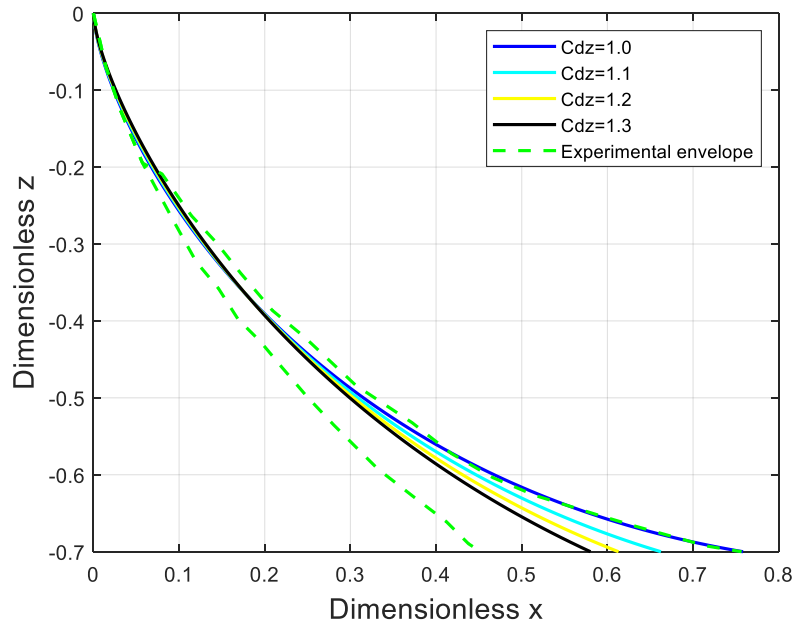


Fig. 10 Simulated dimensionless x-z plane trajectories with different values of C_{dz} at drop angle 60°

Fig. 11 shows time domain dimensionless translational motions in Z direction for initial orientation angle of $\theta_0=45^\circ$ with z direction drag coefficients $C_{dz}=1.0, 1.1, 1.2$ and 1.3 and the trailing edge $Xt=0.4$ is used. The dimensionless translational motions in Z-direction for x direction drag coefficients $C_{dx}=1.0, 1.1, 1.2$ and 1.3 are shown in Fig. 12. For Fig. 12, the trailing edge $Xt=0.4$ is used. In Fig. 12, it can be seen that the deviation of trajectories at different z direction drag coefficients C_{dz} happens in middle of falling motion. The time domain translational motions seem identical for various values of the x direction drag coefficient C_{dx} . Simulation results confirm that the trajectory is significantly affected by the trailing edge.

Figs. 13-15 show the resulting non-dimensional X-Z plane trajectories for the initial orientation angles varying from 0° and 90° in uniform increments of 15° at the trailing edge positions $Xt=0.3, 0.4, \text{ and } 0.5$. The drag coefficient are unchanged with value of $C_{dz}=1.0$ and $C_{dx}=1.2$ for simulations. As shown in Figures, non-dimensional X position tends to increase when increasing the dropped angle up to 60° . When drop angle reach 90° , X tends to decrease to zero. When the trailing edge increase, the positive X position at 90° seems to decrease. Optimal value of trailing edge Xt is 0.4 for drop angle less than 60° and 0.5 for drop angle greater than 60° . The total excursion distribution at non-dimensional z position of 0.7 is employed in the simulation. Non-dimensional simulated results confirm that the initial orientation angle θ_0 is one of the significant factors in determination of shape of trajectories of dropped cylindrical objects, which is consistent with the findings from (Aanesland 1987, Bergmann and Iollo 2011, Luo and Davis 1992).

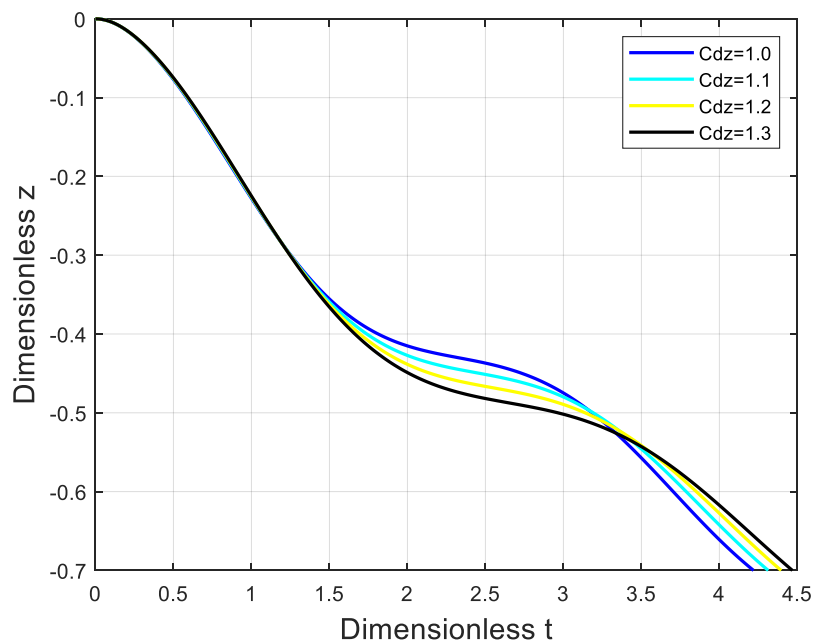


Fig. 11 Simulated time domain dimensionless translational motions in Z-direction with different values of C_{dz}

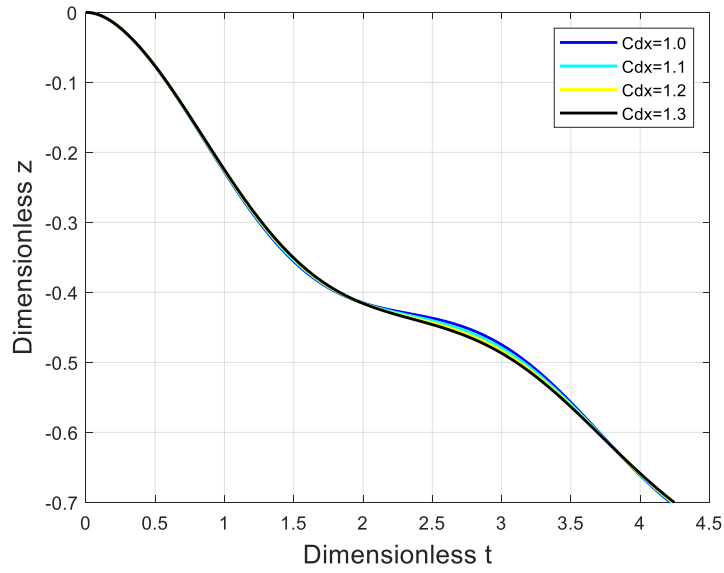


Fig. 12 Simulated time domain dimensionless translational motions in Z-direction with different values of C_{dx}

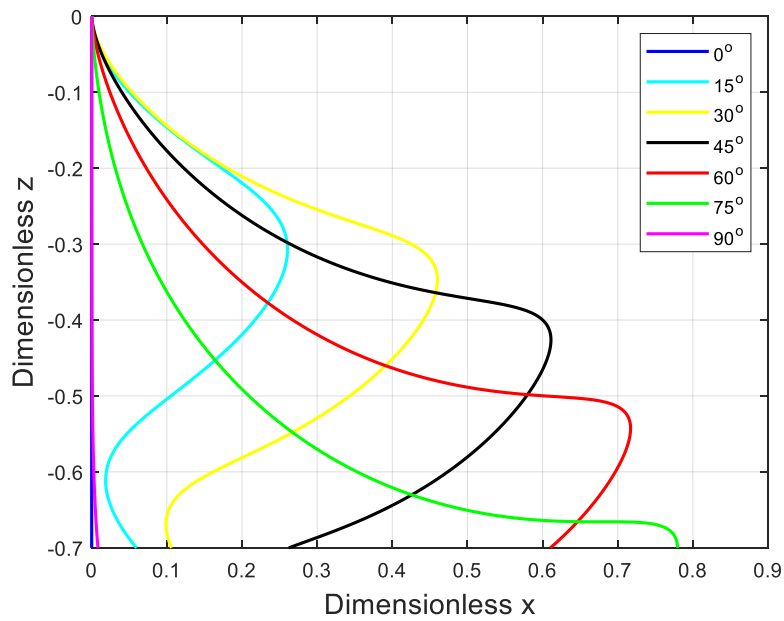


Fig. 13 Simulated dimensionless X-Z plane trajectories with drop angles from 0° to 90° , $Xt=0.3$

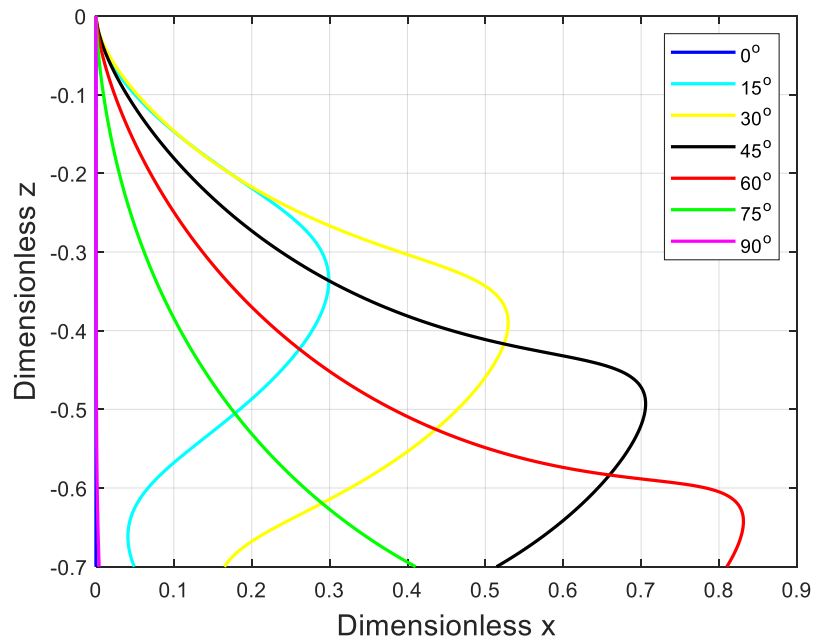


Fig. 14 Simulated dimensionless X-Z plane trajectories with drop angles from 0° to 90°, $X_t=0.4$

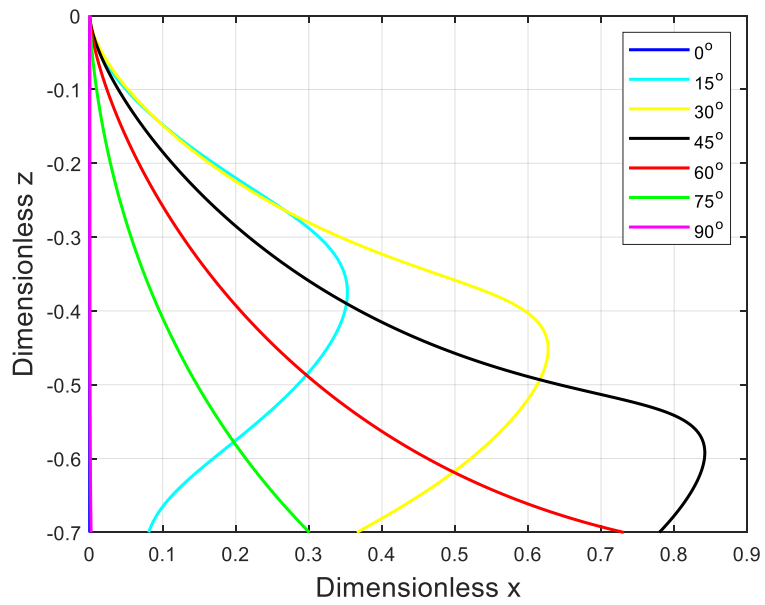


Fig. 15 Simulated dimensionless X-Z plane trajectories with drop angles from 0° to 90°, $X_t=0.5$

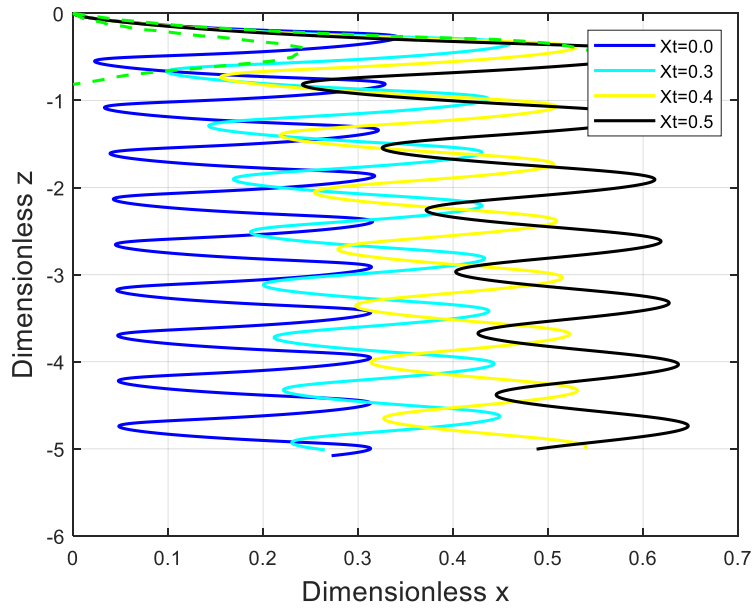


Fig. 16 Simulated dimensionless X-Z plane trajectories at drop angle 30° with dimensionless water depth $z = -5.0$

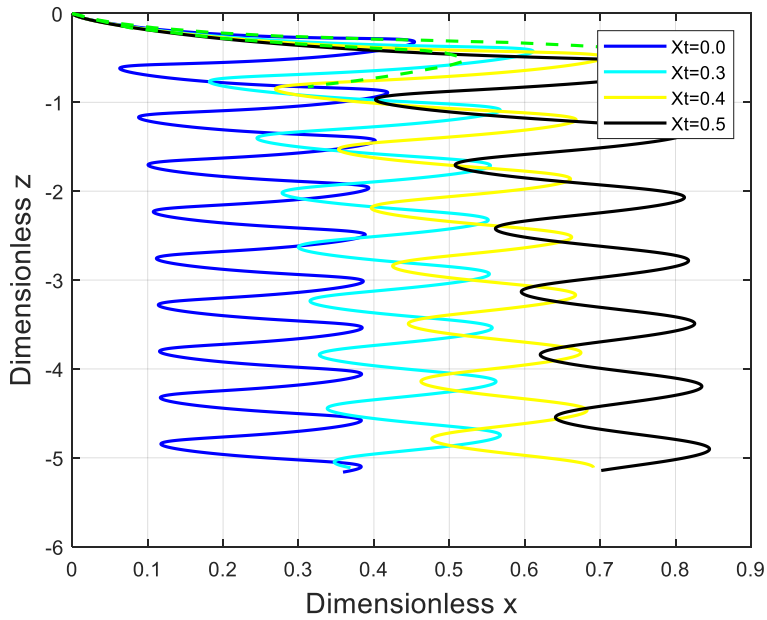


Fig. 17 Simulated dimensionless X-Z plane trajectories at drop angle 45° with dimensionless water depth $z = -5.0$

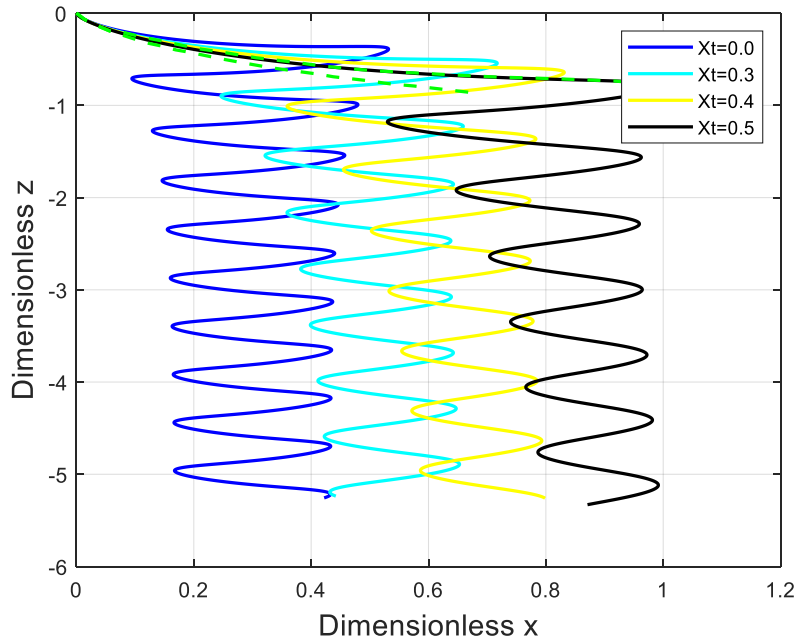


Fig. 18 Simulated dimensionless X-Z plane trajectories at drop angle 60° with dimensionless water depth $z = -5.0$

Figs 16-18 show the resulting dimensionless trajectories in X-Z plane for the initial orientation angles $\theta_0 = 30^\circ, 45^\circ$ and 60° . For each drop angle, the non-dimensional X-Z trajectories have been inspected at three non-dimensional depths of 5. From the Figs. 16-18, the spiral motion or periodic mode in non-dimensional trajectory is largely affected by trailing edge. The increase in trailing edge leads to decreasing in amplitude and frequency of oscillation. At different dropping angles, trajectory exhibits consistent varying pattern of spiral motion.

4. Conclusions

In this paper, the non-dimensionalization is carried out for the two-dimensional coupled surge-heave-pitch motions of dropped cylindrical object, and dimensionless dynamic equations are obtained. Evaluations of dimensionless coefficients of equations of motion show that friction drag is dominant in the surge motion. In addition, the viscous effect and hydrodynamic effect induced by the effective trailing edge on the heave motion are opposite in direction but their magnitudes are in the same level. Furthermore, dropped cylindrical object is subject to substantial influence of moments induced by viscous effect and hydrodynamic effect induced by the effective trailing edge.

Numerical simulation was performed on the dimensionless governing equations of motions. The resulting dimensionless trajectories confirm that trailing edge, the drop angle and z-direction drag coefficient are critical factors which affect the trajectories and the findings are consistent with those

of simulation results (Aanesland 1987, Bergmann and Iollo 2011, Luo and Davis 1992). The initial angle at water-entry greatly affects the underwater trajectory of the dropped cylinder. With increasing initial angle, the larger excursion in x-direction occurs. In addition, it is found that the trailing edge significantly affects the simulated trajectory through the hydrodynamic force upon the object. It is shown that x-directional drag coefficient C_{dx} has little effect on the X-Z plane motion. In addition, as indicated in Figs. 16-18, the trajectories of this cylinder enter a relatively stable steady state after about five cycles. This finding can make it easier to determine the location of landing points.

In future research, proposed dimensionless equations of motion will be used to investigate the revolution of trajectory involving with stochastic noise during process of dynamic motion such as random water entry of dropped object.

References

- Aanesland, V. (1987), Numerical and experimental investigation of accidentally falling drilling pipes. In: 19th Annual OTC in Houston, TX, USA.
- ABS (American Bureau of Shipping) (2013), Guidance notes on accidental load analysis and design for offshore structures. Houston: ABS.
- ABS (American Bureau of Shipping) (2017), Guide for dropped object prevention on offshore units and installations. Houston: ABS.
- Awotahegn, M.B. (2015), Experimental Investigation of Accidental Drops of Drill Pipes and Containers (Master Thesis), University of Stavanger.
- Bergmann, M. and Iollo, A. (2011), "Modeling and simulation of fish-like swimming", *J. Comput. Phys.*, **230**, 329-348
- Colwill, R.D. and Ahilan, R.V. (1992), Reliability analysis of the behavior of dropped objects. In: 24th Annual OTC in Houston, TX, USA
- Chu, P.C., Gilles, A. and Fan, C.W. (2005), "Experiment of falling cylinder through the water column", *Exp. Therm. Fluid Sci.*, **29**, 555-568.
- Chu, P.C. and Fan, C.W. (2006), "Prediction of falling cylinder through air-water-sediment columns", *ASME J. Appl. Mech. Rev.*, **73**, 300-314.
- DNV (Det Norske Veritas) (2010), DNV recommended practice: Risk assessment of pipeline protection. DNV-RP-F107. Oslo, Norway: DNV.
- Dropped Objects Register of Incidents & Statistics (DORIS) (2016), <<http://www.doris.dropsonline.org/>> (accessed 16.03.15)
- Gudmestad, O.T. and Moe, G. (1996), "Hydrodynamic coefficients for calculation of hydrodynamic loads on offshore truss structure", *Mar. Struct.*, **9**(8), 745-758.
- Hoerner, S.F. (1958), Fluid Dynamics Drag, Bricktown, NJ. USA.
- Kim, Y.H., Liu, Y.M. and Yue, D.K.P. (2002), Motion dynamics of three-dimensional bodies falling through water. In: 17th IWWFEB, 21-081.
- Luo, Y. and Davis, J. (1992), Motion simulation and hazard assessment of dropped objects, In: Proceedings of the Second International Offshore and Polar Engineering Conference, ISBN 1-880653-04-4(Vol IV), San Francisco, USA
- Majed, A. and Cooper, P. (2013), "High Fidelity Sink Trajectory Nonlinear Simulations for Dropped Subsea Objects", *Proceedings of the 23rd Int Offshore Polar Eng. Conf, Anchorage, AK, USA, ISOPE, 2, 18-26.*
- Newman, J.N. (1977), Marine Hydrodynamic, The MIT Press, Cambridge, Massachusetts, USA.
- Schlichting, H. (1979), Boundary Layer Theory. McGraw-Hill Book Company, New York, USA.
- Xiang, G., Birk, L., Li, L., Yu, X. and Luo, Y. (2016), "Risk free zone study for cylindrical objects dropped into the water", *J. Ocean Syst. Eng.*, **6**(4), 377-400.

- Xiang, G., Birk, L., Yu, X. and Li, X. (2017a), "Study of the trajectory and landing points of dropped cylindrical object with different longitudinal center of gravity", *Int. Soc. Offshore Polar Engineers*, **27**(3), 274-282.
- Xiang, G., Birk, L., Yu, X. and Lu, H., (2017b), "Numerical study on the trajectory of dropped cylindrical objects", *J. Ocean Eng.*, **130**, 1-9.
- Yasseri, S. (2014), "Experimental of free-falling cylinders in water", *Underwater Technol.*, **32**(2), 177-191.
- Yu, X., Li, L., Xiong, Z. and Kang, S. (2020a), "Hit probability of cylindrical objects dropped on pipelines in offshore operations", *J. Pipeline Systems - Engineering and Practice*, **11**(4), 04020048.
- Yu, X., Xiang, G., Collopy, H. and Kong, X. (2020b), "Trajectory tracking of a model rocket falling into the towing tank: Experimental tests versus numerical simulations", *J. Aerosp. Eng.*, **33**(5), 04020056.

MK